Stability of vicinal metal surfaces: From semi-empirical potentials to electronic structure calculations

F. Raouafi,[1] C. Barreteau,[1] D. Spanjaard,[2] and M. C. Desjonquères[1]
[1]*DSM/DRECAM/SPCSI, CEA Saclay F-91 191 Gif sur Yvette, France*
[2]*Laboratoire de Physique des Solides, Université Paris Sud, F-91 405 Orsay, France*
(Received 27 March 2002; published 19 July 2002)

The stability of metal vicinal surfaces with respect to faceting is investigated using pair potentials, semi-empirical potentials, and tight-binding electronic structure calculations for several domains of orientations. It is proven that pair potentials are not precise enough to determine the stability of these surfaces. The answer obtained with semi-empirical potentials is shown to be quite sensitive to the cutoff distance chosen for the interactions and may be too schematic. The results derived from electronic structure calculations open up the possibility of a larger diversity of behaviors due to the existence of electronic step-step interactions. Finally it is shown that the effects of temperature are quite small, at least up to room temperature.

DOI: 10.1103/PhysRevB.66.045410 PACS number(s): 68.35.Md, 65.40.Gr, 68.35.Ja, 68.35.Rh

I. INTRODUCTION

A vicinal surface is a surface of high Miller indices and exhibits a periodic succession of terraces and steps of monoatomic height. The study of these surfaces is presently the subject of intensive investigations since they may provide an appropriate substrate for growing nanostructures.[1,2] However, these surfaces are not always stable. Indeed, it might be energetically favorable for the system to increase its total area in order to expose to vacuum facets with low Miller indices with smaller surface energies per unit area. These faceted surfaces may also be interesting to elaborate nanostructures since atoms deposited on these surfaces will preferentially occupy sites in the inner edges in order to maximize their coordination. This may lead to a periodic lattice of nanowires with magnetic and transport properties of high technological interest.

Up to now, in spite of the large number of experiments carried out on these surfaces,[3–7] very few theoretical works based on an atomistic description have been devoted to this problem. The faceting condition implies the calculation of the surface energy for any surface orientation. There exist several ways of computing these energies. The most simple of them use potentials ranging from the crudest empirical pair potentials to semi-empirical ones[8] including an *N*-body contribution. In the latter case the analytical expression of the semi-empirical potentials attempts to mimic the results of more accurate methods based on the calculation of the electronic structure such as the tight-binding approximation or first-principle methods based on the density-functional theory. The latter two methods, in which the electronic structure is explicitly calculated, can also be used. However, in view of the large size of the unit cells of vicinal surfaces with wide terraces, systematic calculations can be carried out only within the tight-binding method.[9,10]

The aim of this paper is to discuss the implications of these different approaches on the stability of vicinal surfaces relative to faceting. Preliminary results of this work have already been presented in Ref. 11 concerning the faceting of the vicinal surfaces found between the (100) and (111) planes into (100)/(111) facets. In the present study we examine the problem in more detail and consider different domains of orientations.

The paper is organized as follows. In Sec. II the faceting condition is established and the geometry of the vicinal surfaces involved in these domains is explained. In Sec. III the stability of these vicinal surfaces is analyzed using different (semi)-empirical potentials. Analytical results are first derived for a rigid lattice and an application to vicinal surfaces of copper, including surface relaxation, is presented using a semi-empirical potential of the tight-binding type[12] with a particular emphasis on the importance of the cutoff radius chosen for atomic interactions. The results of electronic structure calculations based on the tight-binding approximation using a s,p,d orbital basis set on a rigid lattice are then discussed in Sec. IV for rhodium, palladium, and copper. The effects of temperature are studied in Sec. V for copper. Finally conclusions are drawn in Sec. VI.

II. FACETING CONDITION OF AN INFINITE SURFACE

Let us consider two low index surfaces Σ_1 and Σ_2 with normals $\mathbf{n}_1$ and $\mathbf{n}_2$, respectively, which intersect along a given row of atoms and the set of vicinal surfaces with equidistant step edges which is spanned when Σ_1 is rotated around the common atomic row towards Σ_2. Let us take Σ_1 as the origin of angles and denote θ_2 the angle $(\mathbf{n}_1, \mathbf{n}_2)$. During this rotation the surfaces vicinal to Σ_1 are first found and the number of atomic rows p_1 (including the inner edge) on one terrace decreases from ∞ to 2 (angle θ_c). The surface corresponding to θ_c can also be regarded as a vicinal of Σ_2 with $p_2=2$. Then for $\theta_c \leqslant \theta < \theta_2$ the surfaces vicinal to Σ_2 are scanned with increasing terrace widths ($p_2 \geqslant 2$). An area S of any of these high index surfaces will transform into facets of normal $\mathbf{n}_1$ (area S_1) and normal $\mathbf{n}_2$ (area S_2) while keeping its average orientation when (Fig. 1)

$$\gamma S > \gamma_1 S_1 + \gamma_2 S_2 \tag{1}$$

(γ, γ_1 and γ_2 being the surface energies per unit area of the high index, Σ_1 and Σ_2 surfaces, respectively) with the constraints

 ©2002 The American Physical Society

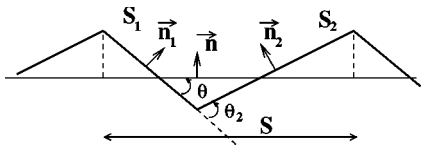

FIG. 1. Faceting.

$$S = S_1 \cos\theta + S_2 \cos(\theta_2 - \theta), \tag{2}$$

$$S_1 \sin\theta = S_2 \sin(\theta_2 - \theta). \tag{3}$$

It is easily shown that the faceting condition can be written

$$f(\eta) > (1-\eta/\eta_2) f(0) + (\eta/\eta_2) f(\eta_2) \tag{4}$$

with $\eta = \tan\theta$ and $f(\eta) = \gamma(\theta)/\cos\theta$. This condition is equivalent to the Herring[13] construction (see Appendix A).

This condition has a simple geometrical interpretation: the point $(\eta, f(\eta))$ must be above the straight line D joining the points $(0, f(0))$ and $(\eta_2, f(\eta_2))$ or, equivalently, the sign of the deviation $\Delta f(\eta)$ from this straight line determines the stability $[\Delta f(\eta) < 0]$ or the instability $[\Delta f(\eta) > 0]$ of the vicinal surface. It can be easily shown (see Appendix B) that

$$\Delta f(\mathbf{n}) = [E_S(\mathbf{n}) - (p_1 - 1) E_S(\mathbf{n}_1) - (p_2 - 1) E_S(\mathbf{n}_2)]/A_0(\mathbf{n}), \tag{5}$$

where $A_0(\mathbf{n})$ is the projected area of the surface unit cell A of the vicinal surface of orientation $\mathbf{n}$ on Σ_1. This formula applies as well in the domain $0 \leqslant \theta \leqslant \theta_c$ with $p_2 = 2$, as when $\theta_c \leqslant \theta \leqslant \theta_2$ with $p_1 = 2$. $E_S(\mathbf{n})$ is the surface energy (per atom) of the surface normal to $\mathbf{n}$. It is interesting to note that the condition of instability of the surface corresponding to η_c (normal $\mathbf{n_c}$) is simply

$$E_S(\mathbf{n}_c) > E_S(\mathbf{n}_1) + E_S(\mathbf{n}_2); \tag{6}$$

we will see below that in many cases the sign of $\Delta f(\eta_c)$ determines the stability for the whole range $[0, \eta_2]$. It is clear that the sign of Δf is independent of the origin of angles, i.e., if Σ_1 is referred by the angle θ_1, since it is given by the sign of the expression between the square brackets in Eq. (5) which will be denoted as $\Delta E(p_1, p_2)$ in the following.

Let us denote A_1 (A_2) the area of the unit cell of Σ_1 (Σ_2). It is straightforward to show that

$$\begin{cases} \Delta f(\eta) = \dfrac{\Delta E(p_1,2)}{A_2 \sin\theta_2}\,\eta, & 0 \leqslant \eta \leqslant \eta_c, \\ \Delta f(\eta) = \dfrac{\Delta E(2,p_2)}{A_1}(1-\eta/\eta_2), & \eta_c \leqslant \eta \leqslant \eta_2. \end{cases} \tag{7}$$

The expression for ΔE can be transformed using the formula given by Vitos *et al.*[14] for the step energy, i.e.,

$$E_{step}(\mathbf{n_i}, p_i) = E_S(\mathbf{n_i}, p_i) - (p_i - 1 + f_i) E_S(\mathbf{n_i}), \tag{8}$$

where $E_{step}(\mathbf{n_i}, p_i)$ is the step energy (per step atom) in the vicinal surface the terraces of which are normal to $\mathbf{n_i}$ and have p_i atomic rows. $E_S(\mathbf{n_i}, p_i)$ is the surface energy per atom of this vicinal surface which was equivalently denoted as $E_S(\mathbf{n})$ in Eq. (5). Finally f_i is a geometrical factor which is equal to the ratio of the area, projected on the terrace, of the unit cell of the ledge to the area of the unit cell of the terrace $[f_1 = A_2\cos(\theta_2)/A_1,\ f_2 = A_1\cos(\theta_2)/A_2]$. Substituting for $E_S(\mathbf{n_i}, p_i)$ from Eq. (8) into $\Delta E(p_1, 2)$, for instance, yields

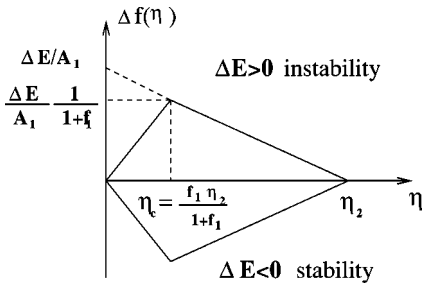

FIG. 2. Behavior of $\Delta f(\eta)$ when there are no interactions between steps. η_c corresponds to $p_1 = p_2 = 2$.

$$\Delta E(p_1, 2) = E_{step}(\mathbf{n}_1, p_1) - E_S(\mathbf{n}_2) + f_1 E_S(\mathbf{n}_1); \tag{9}$$

a similar equation can be written for $\Delta E(2, p_2)$ by interchanging the indices 1 and 2 in the right-hand side of Eq. (9). Note that, due to the continuity of $\Delta f(\eta)$ at η_c ($p_1 = p_2 = 2$), the following relation holds:

$$E_{step}(\mathbf{n}_1, 2) - E_{step}(\mathbf{n}_2, 2) = (1+f_2) E_S(\mathbf{n}_2) - (1+f_1) E_S(\mathbf{n}_1). \tag{10}$$

If we note that when, in a first approach, we assume that the contribution of the ledge to the surface energy of the vicinal surface can be approximated by the corresponding macroscopic surface energy, then ΔE vanishes. Thus ΔE is a measure of the deviation to this approximation. Rigorously, ΔE does not vanish and is a function of η since $E_{step}(\mathbf{n_i}, p_i)$ depends on p_i due to step-step interactions.

When these interactions are neglected $\Delta E(p_1, 2)$ and $\Delta E(2, p_2)$ are equal to the same constant ΔE since they must be equal for $\eta = \eta_c$. When ΔE is not vanishing $\Delta f(\eta)$ has a triangular shape [see Eq. (7)] and both quantities have the same sign (see Fig. 2). In the particular case $\Delta E = 0$, any vicinal surface between Σ_1 and Σ_2 has the same energy as the corresponding faceted surface.

Actually, this simple picture is modified by the interactions between steps even at 0 K. When neglecting relaxation, steps start to interact when the range of the potential is large enough. Then the two straight lines of Fig. 2 transform into as many segments (with discontinuities of slope) as there are different step energies when p increases. In addition, in calculations based on the determination of the electronic structure, long-range oscillatory interactions are present.[9,10] Finally, atomic relaxation introduces step-step repulsive interactions which tends to lower $\Delta f(\eta)$ and to give it a positive curvature in both domains ($0 \leqslant \eta \leqslant \eta_c$, $\eta_c \leqslant \eta \leqslant \eta_2$). In the next sections the stability of vicinal surfaces is analyzed using different methods giving the total energy

ranging from pair potentials, semi-empirical potentials including an N-body contribution, and, finally, electronic structure calculations. Then we will study the effects of temperature.

Let us finally remark that the curvature of $f(\eta)$ has the same sign as $\gamma(\theta)+d^2\gamma/d\theta^2$ since

$$\frac{d^2f}{d\eta^2}=\frac{d^2[\gamma(\theta)/\cos\theta]}{(d\tan\theta)^2}=\cos^3\theta[\gamma(\theta)+d^2\gamma/d\theta^2] \quad (11)$$

with $0\leqslant\theta<\pi/2$. It is well known that when $\gamma(\theta)+d^2\gamma/d\theta^2\leqslant 0$, the surface orientation θ is unstable and will minimize its energy by developing facets. Therefore in the domain of η where $d^2f/d\eta^2$ is negative, the corresponding surfaces are unstable. Otherwise they are stable or metastable.[15]

III. STABILITY OF VICINAL SURFACES AT 0 K FROM SEMI-EMPIRICAL POTENTIALS

Empirical potentials belonging to a very large class can be written as a sum of contributions E_i of each atom i (the origin of energy being the energy of a free atom so that $E_i<0$) depending on its environment of neighbors j at the interatomic distance R_{ij}, i.e.,

$$E=\sum_i E_i=\sum_i\left[\sum_{j\neq i}V(R_{ij})+F\left(\sum_{j\neq i}g(R_{ij})\right)\right]. \quad (12)$$

E is the total energy of the system at 0 K neglecting the zero-point vibrational energy. In the following we set $\rho_i=\Sigma_{j\neq i}g(R_{ij})$. The first term of Eq. (12) is thus pairwise while the second one (in which g is a positive function) has an N-body character. The functions V and g are usually cutoff smoothly around a given radius R_c. This class of potentials includes pair potentials [$F(\rho_i)=0$], potentials based on effective medium theory (EMT),[16,17] embedded atom model (EAM),[18] and glue model,[19] and potentials derived from the tight-binding approximation in the second moment approach [$F(\rho_i)\propto\sqrt{\rho_i}$],[20–23] or fitted to calculations including higher-order moments [$F(\rho_i)\propto\rho_i^{2/3}$].[12,24] Note that in potentials of the tight-binding type, the N-body part is strictly attractive while the pairwise part is strictly repulsive.

We first fix the interatomic distances to their bulk equilibrium values, i.e., atomic relaxation effects are ignored. With this assumption $\Sigma_{j\neq i}V(R_{ij})$ and $\Sigma_{j\neq i}g(R_{ij})$ are linear combinations of the number of neighbors Z_N^i of atom i in the Nth coordination sphere of radius R_N ($R_N<R_c$) and $E_i=E(Z_1^i\cdots Z_N^i\cdots)$. It is usual to take R_1 as the reference distance and set $g(R_1)=1$.

To proceed further we must specify the set of vicinal surfaces we want to study. We limit ourselves to fcc crystals and consider here two domains (Fig. 3). The first domain is defined by $\mathbf{n}_1=(1,0,0)$ and $\mathbf{n}_2=(1,1,1)$. In this domain, when $0<\eta\leqslant\eta_c(\eta_c=\sqrt{2}/3)$ the crystallographic planes $(2p-1,1,1)$ are spanned and correspond to the $p(100)\times(111)$ surfaces in Somorjai notations[25] and when $\eta_c\leqslant\eta<\eta_2$ ($\eta_2=\sqrt{2}$) the crystallographic planes are $(p+1,p-1,p-1)$ and

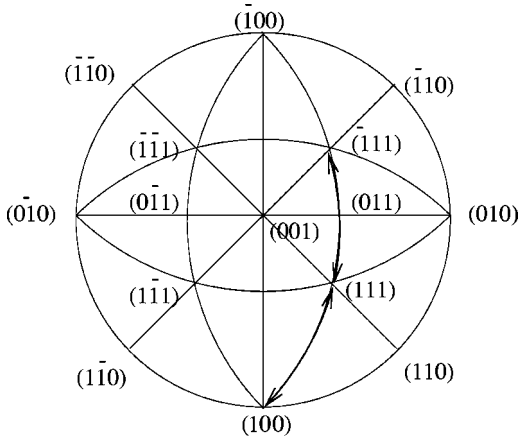

FIG. 3. Stereographic projection of the two ranges of orientations studied (heavy lines).

the corresponding vicinal surfaces are $p(111)\times(100)$. Note that for $\eta=\eta_c$ the Miller indices of the surface are (311).

The second domain that we will study is the domain of vicinals between $(1\bar{1}1)$ and (111), i.e., $p(1\bar{1}1)\times(111)$ [with Miller indices $(2-p,p,p)$] and $p(111)\times(1\bar{1}1)$ [with Miller indices $(p-2,p,p)$]. The surface corresponding to η_c ($p=2$) is (011). This domain being symmetrical with respect to the (011) surface we take the origin of angles at this surface, i.e., $\eta_c=0$, thus $\eta\in[-\eta_2,\eta_2]$ with $\eta_2=\sqrt{2}/2$. This range is interesting since, in particular, it will give information on the possibility of faceting of the (011) surface into $(1\bar{1}1)$ and (111) facets. Indeed the missing row reconstruction which is observed at the (011) surface of some fcc transition metals[26] can be viewed as a ''microscopic'' faceting of this type. Let us consider in more detail the interval $[0,\eta_2]$: the surfaces that are first spanned are the $p(011)\times(111)$ vicinal surfaces [with Miller indices $(1,2p-1,2p-1)$] until $p=2$, i.e., the (133) surface [$\eta_c=\sqrt{2}/6$]. Then the surfaces between (133) and (111) are $p(111)\times(011)$ or $(p-1,p+1,p+1)$ which have the same geometry as the $(p+1)(111)\times(1\bar{1}1)$ surface since the choice of the ledge is somewhat arbitrary (note that the number of rows being increased by 1 in the last case, the corresponding geometrical factor f should be decreased by 1). Thus the study of $\Delta f(\eta)$ between 0 and η_2 will give the stability of these vicinal surfaces with respect to faceting into (011) and (111) facets.

The geometry of the studied surfaces being now defined, it is easy to determine the coordination numbers $Z_1^i,Z_2^i,\cdots Z_N^i\cdots$ for the successive atomic layers i of any surface. The values of f and these coordination numbers are given in Tables I –Vfor each surface up to $N=5$ since interactions are very rapidly screened in metals. The last atomic layer of each surface refers to the first layer which has the same first five coordination numbers as a bulk atom. In the next two subsections we first discuss the case of pair potentials and then the influence of the contribution of an N-body term. In all cases, assuming a rigid lattice, we will determine the largest range R_{max} of the potential for which the step energies remain a constant for $p\geqslant 2$ for both types of steps involved in the considered domain. Then we limit ourselves to ranges

TABLE I. Coordination numbers Z_N in the Nth coordination sphere of atoms belonging to successive atomic layers for the (111), (100), and (011) fcc surfaces up to the first layer in which atoms have the same first five coordination numbers as a bulk atom. $n^N(\infty)$ is the total number of Nth neighbors (per surface atom) suppressed by the surface.

(111) surface					
Layer	Z_1	Z_2	Z_3	Z_4	Z_5
1	9	3	15	9	12
2	12	6	21	9	18
3	12	6	24	12	24
$n^N(\infty)$	3	3	12	6	18
(100) surface					
Layer	Z_1	Z_2	Z_3	Z_4	Z_5
1	8	5	12	8	16
2	12	5	20	8	20
3	12	6	24	12	20
4	12	6	24	12	24
$n^N(\infty)$	4	2	16	8	16
(011) surface					
Layer	Z_1	Z_2	Z_3	Z_4	Z_5
1	7	4	14	7	12
2	11	4	18	7	16
3	12	6	20	11	18
4	12	6	24	11	22
5	12	6	24	12	24
$n^N(\infty)$	6	4	20	12	28

$R_c \leqslant R_{max}$ in which case $\Delta f(\eta)$ has a triangular shape and examine its sign given by ΔE (Fig. 2). We will end by a numerical study of Cu vicinal surfaces using a potential of the tight-binding type, discussing the influence of relaxation and of the position of the cutoff R_c.

A. Pair potentials

These potentials are the simplest ones which have been used in the past. We will limit ourselves to the study of unrelaxed surfaces since it is well known that they most often lead to an outward relaxation instead of the inward one generally observed at metal surfaces. However, such pair interactions V_N between an atom and one of its neighbors in the Nth coordination shell have been used on a rigid lattice by Vitos *et al.*[14] in order to estimate step energies in transition and noble metals and study the stability of the fcc(011) surfaces.[27] From Eq. (8) it is seen that

$$E_{step}(p) = \sum_{R_N < R_c} n^N_{step}(p) V_N \tag{13}$$

with

$$n^N_{step}(p) = n^N_{vici}(p) - (p - 1 + f) n^N(\infty), \tag{14}$$

where $n^N_{vici}(p)$ and $n^N(\infty)$ are, respectively, the total number of neighbors in the Nth coordination shell suppressed by the vicinal surface with p atomic rows on the terraces and by the flat surface parallel to the terrace. In Eq. (13) the sign of V_N is defined in such a way that the energy of a bulk atom is written $E_{bulk} = -\Sigma_{R_N < R_c} Z^b_N V_N$ where Z^b_N is the number of Nth neighbors for a bulk atom and the surface energy is $E_S = \Sigma_{R_N < R_c} n^N_S V_N$ where n^N_S is the total number of Nth neighbors (per surface atom) suppressed by the surface.

There are no interactions between steps as long as $n^N_{step}(p)$ does not depend on $p (p \geqslant 2)$. We will see in the following that this condition is fulfilled only when R_c is

TABLE II. Same caption as Table I for the $p(100)\times(111)$ or $(2p-1,1,1)$ vicinal surfaces ($f = 1/2$). n^N_{vici} is the total number of Nth neighbors (per surface atom) suppressed by the surface. The values of n^N_{step} which determine the step energies in the pair potential model of Vitos *et al.* (Ref. 14) are also given.

$p=2$, (311) surface					
Layer	Z_1	Z_2	Z_3	Z_4	Z_5
1	7	3	14	7	14
2	10	5	16	7	16
3	12	5	19	10	18
4	12	6	23	10	20
5	12	6	24	12	22
6	12	6	24	12	24
n^N_{vici}	7	5	24	14	30
n^N_{step}	1	2	0	2	6
$p=3$, (511) surface					
Layer	Z_1	Z_2	Z_3	Z_4	Z_5
1	7	3	12	7	12
2	8	5	14	7	16
3	10	5	16	8	18
4	12	5	18	8	18
5	12	5	21	10	20
6	12	6	23	10	20
7	12	6	24	12	20
8	12	6	24	12	22
9	12	6	24	12	24
n^N_{vici}	11	7	40	22	46
n^N_{step}	1	2	0	2	6
$p=4$, (711) surface					
Layer	Z_1	Z_2	Z_3	Z_4	Z_5
1	7	3	12	7	12
2	8	5	12	7	14
3	8	5	14	8	18
4	10	5	16	8	18
5	12	5	18	8	18
6	12	5	20	8	20
7	12	5	21	10	20
8	12	6	23	10	20
9	12	6	24	12	20
10	12	6	24	12	20
11	12	6	24	12	22
12	12	6	24	12	24
n^N_{vici}	15	9	56	30	62
n^N_{step}	1	2	0	2	6

TABLE III. Same caption as Table II for the $p(111)\times(100)$ or $(p+1,p-1,p-1)$ vicinal surfaces ($f=2/3$). For $p=2$, see the (311) surface in Table II but n^N_{step} should be replaced by (2, 0, 4, 4, 0).

			$p=3$, (211) surface		
Layer	Z_1	Z_2	Z_3	Z_4	Z_5
1	7	3	12	7	12
2	9	3	16	7	14
3	10	5	17	9	16
4	12	5	19	9	16
5	12	6	21	10	18
6	12	6	23	10	22
7	12	6	24	12	22
8	12	6	24	12	24
n^N_{vici}	10	8	36	20	48
n^N_{step}	2	0	4	4	0
			$p=4$, (533) surface		
Layer	Z_1	Z_2	Z_3	Z_4	Z_5
1	7	3	12	7	12
2	9	3	14	7	12
3	9	3	17	9	14
4	10	5	17	9	16
5	12	5	19	9	16
6	12	6	21	9	16
7	12	6	21	10	20
8	12	6	23	10	22
9	12	6	24	12	22
10	12	6	24	12	24
n^N_{vici}	13	11	48	26	66
n^N_{step}	2	0	4	4	0

small enough. Then, $\Delta f(\eta)$ is linear in both domains $[0,\eta_c]$ and $[\eta_c,\eta_2]$. However, depending on the range of the potential, either these two straight lines join at η_c with a discontinuity of slope, or $\Delta f(\eta)=0$ when $\eta\in[0,\eta_2]$. In the former case, the sign of $\Delta f(\eta_c)$ is sufficient to know whether the vicinal surfaces are stable or not.

1. $p(100)\times(111)$-$p(111)\times(100)$ domain

From Tables II and III it is seen that $E^{p(100)\times(111)}_{step}$ and $E^{p(111)\times(100)}_{step}$ are independent of p when the pair interactions do not reach the sixth neighbors (actually they begin to depend on p when the pair interactions reach the seventh and sixth neighbors, respectively). Let us thus assume that the pair interactions are cut beyond the fifth neighbors and determine the sign of ΔE from Eq. (5) and Tables I and II. We find

$$\Delta E=E_S(311)-E_S(100)-E_S(111)=-4(V_3+V_5). \tag{15}$$

As a conclusion, if the range of the pair potential is limited to the first and second neighbors $\Delta E=0$, so that the energy of any vicinal surface is equal to the energy of the faceted (100)/(111) surface. If the range is extended to fifth

TABLE IV. Same caption as Table II for the $p(111)\times(\bar{1}11)$ or $(p-2,p,p)$ vicinal surfaces ($f=1/3$). The same table can be used for $(p-1)(111)\times(011)$ ($f=4/3$) (see the main text).

			$p=2$, (011) surface		
Layer	Z_1	Z_2	Z_3	Z_4	Z_5
1	7	4	14	7	12
2	11	4	18	7	16
3	12	6	20	11	18
4	12	6	24	11	22
5	12	6	24	12	24
n^N_{vici}	6	4	20	12	28
n^N_{step}	2	0	4	4	4
			$p=3$, (133) surface		
Layer	Z_1	Z_2	Z_3	Z_4	Z_5
1	7	3	12	7	14
2	9	4	16	7	14
3	11	4	19	9	14
4	12	6	19	9	18
5	12	6	22	11	20
6	12	6	24	11	22
7	12	6	24	12	24
n^N_{vici}	9	7	32	18	42
n^N_{step}	2	0	4	4	0
			$p=4$, (122) surface		
Layer	Z_1	Z_2	Z_3	Z_4	Z_5
1	7	3	12	7	12
2	9	3	14	7	14
3	9	4	17	9	14
4	11	4	19	9	14
5	12	6	19	9	16
6	12	6	21	9	20
7	12	6	22	11	20
8	12	6	24	11	22
9	12	6	24	12	24
n^N_{vici}	12	10	44	24	60
n^N_{step}	2	0	4	4	0
			$p=5$, (355) surface		
Layer	Z_1	Z_2	Z_3	Z_4	Z_5
1	7	3	12	7	12
2	9	3	14	7	12
3	9	3	15	9	14
4	9	4	17	9	14
5	11	4	19	9	14
6	12	6	19	9	16
7	12	6	21	9	18
8	12	6	21	9	20
9	12	6	22	11	20
10	12	6	24	11	22
11	12	6	24	12	24
n^N_{vici}	15	13	56	30	78
n^N_{step}	2	0	4	4	0

TABLE V. Same caption as Table II for the $p(011)\times(111)$ or $(1,2p-1,2p-1)$ vicinal surfaces ($f=1/2$). For $p=2$, see Table IV for the (133) surface, but n^N_{step} should be replaced by (0,1,2,0,0).

$p=3$, (155) surface					
Layer	Z_1	Z_2	Z_3	Z_4	Z_5
1	7	3	12	7	12
2	7	4	14	7	14
3	9	4	16	7	14
4	11	4	18	7	14
5	11	4	19	9	16
6	12	6	19	9	18
7	12	6	20	11	18
8	12	6	22	11	20
9	12	6	24	11	22
10	12	6	24	11	22
11	12	6	24	12	24
n^N_{vici}	15	11	52	30	70
n^N_{step}	0	1	2	0	0
$p=4$, (177) surface					
Layer	Z_1	Z_2	Z_3	Z_4	Z_5
1	7	3	12	7	12
2	7	4	14	7	12
3	7	4	14	7	14
4	9	4	16	7	14
5	11	4	18	7	14
6	11	4	18	7	16
7	11	4	19	9	16
8	12	6	19	9	18
9	12	6	20	11	18
10	12	6	20	11	18
11	12	6	22	11	20
12	12	6	24	11	22
13	12	6	24	11	22
14	12	6	24	11	22
15	12	6	24	12	24
n^N_{vici}	21	15	72	42	98
n^N_{step}	0	1	2	0	0

neighbors the surface is stable if $V_3+V_5<0$ and unstable otherwise. Then $\Delta f(\eta)$ behaves as shown in Fig. 2. If we look at the numerical values of V_3 given by Vitos *et al.*[14] when $R_3<R_c<R_4$, the only element for which V_3 is negative is Au, but it is well known that Au(100) and Au(111) reconstruct and thus the present analysis, which assumes unreconstructed flat surfaces, cannot be applied.

2. $p(\bar{1}\bar{1}\bar{1})\times(111)$-$p(111)\times(\bar{1}\bar{1}\bar{1})$ *domain*

In this domain, as already stated, we choose θ_c as the origin of angles ($\eta_c=0$) and $\eta\in[-\eta_2,\eta_2]$ with $\eta_2=\sqrt{2}/2$. In these conditions D is the horizontal line at ordinate $f(\eta_2)=\gamma(111)/\cos\theta_2$. The corresponding steps do not interact as long as $R_c<R_5$ (see Table IV). Then $\Delta f(\eta)$ has a triangular shape and the position of its apex relative to the η axis determines the stability of the vicinal surfaces. From Eq. (6) they are unstable when

$$\Delta E=E_S(011)-2E_S(111)>0, \tag{16}$$

i.e., when $V_2+2V_3<0$ and stable otherwise. Note that in the former case, the step energy (V_2+2V_3) of the $p(011)\times(111)$ is negative and the (011) surface is less stable than the missing row reconstructed $(011)(2\times1)$ surface.[10,14] All these findings are consistent with an instability of the (011) surface when $V_2+2V_3<0$. The latter condition is not fulfilled for the fcc elements of the $3d$ and $4d$ transition-metal series when using the pair interactions given by Vitos *et al.*, in accordance with the stability of the (011) surface of these elements. For Pt and Au, V_2+2V_3 is negative and this would be consistent with the missing row reconstruction occurring for both elements. However, we must note that the condition (16) is not really applicable for Au(111) since this surface is reconstructed. The case of Ir(011) is still under debate since V_2+2V_3 is positive according to Ref. 14 and very close to 0 from Ref. 27.

3. $p(011)\times(111)$-$p(111)\times(011)$ *domain*

This domain is defined by $\eta\in[0,\sqrt{2}/2]$. The surface $p=2$ corresponding to $\eta_c=\sqrt{2}/6$ is the (133) crystallographic plane. From Tables IV and V we see that, when $R_c<R_6$ at least, the step energies $E^{p(011)\times(111)}_{step}$ and $E^{p(111)\times(011)}_{step}$ are independent of p (actually, steps begin to interact when $R_c>R_{12}$ for the first ones, and $R_c>R_8$ for the second ones![28]). From Eq. (6) these vicinal surfaces are unstable with respect to faceting into (011)-(111) facets when

$$E_S(133)>E_S(011)+E_S(111). \tag{17}$$

This inequality is fulfilled when $V_5<0$ if $R_c<R_6$. As a consequence when $R_c<R_5$, all vicinal surfaces in this domain are degenerate with the faceted ones. If $R_c<R_6$ and $V_5\neq0$, $\Delta f(\eta)$ has the triangular shapes shown in Fig. 2 with $\Delta E>0$ ($V_5<0$) and $\Delta E<0$ ($V_5>0$).

Let us now summarize our results. We have found that the faceted surface is nondegenerate with the vicinal one when the pair potential includes third neighbors for the (100)-(111) domain, second neighbors for the $(\bar{1}\bar{1}1)$-(111) domain, and fifth neighbors for the (011)-(111) domain. However, we have shown in a recent work[10] that pair potentials derived from *ab initio* calculations of surface energies are very dependent of the used data base, in particular even the sign of V_2 is uncertain. Thus the use of pair potentials to study the faceting of metal surfaces is questionable.

B. *N*-body semi-empirical potentials

Let us now examine the case of semi-empirical potentials including an *N*-body contribution. We will first neglect atomic relaxation and derive general trends for potentials of type (12). Then we will present examples of the use of such a semi-empirical potential in the case of Cu vicinal surfaces without and with relaxation.

1. Case of rigid lattices

Here the interatomic distances are fixed to their bulk equilibrium values and, as stated above, the energy of an atom i

is completely determined by its coordination numbers up to the cutoff radius, i.e., $E_i = E(Z_1^i, \cdots Z_N^i)$.

(a) $p(100)\times(111)$-$p(111)\times(100)$ domain. We limit ourselves to values of R_c such that $R_c < R_4$ since, as we will see below, $\Delta f(\eta)$ deviates from the triangular shape as soon as R_c reaches the third neighbors. Let us first examine when $E_{step}^{p(100)\times(111)}$ is independent of p. Using Tables I, II, and III and Eq. (8) we find

$$E_{step}^{2(100)\times(111)} = E(7,3,14) - 3E(8,5,12)/2 + E(10,5,16) + E(12,5,19) - 3E(12,5,20)/2 + E(12,6,23) - E(12,6,24) \quad (18)$$

and

$$E_{step}^{3(100)\times(111)} = E(7,3,12) - 5E(8,5,12)/2 + E(8,5,14) + E(10,5,16) + E(12,5,18) - 5E(12,5,20)/2 + E(12,5,21) + E(12,6,23) - E(12,6,24). \quad (19)$$

It is easily seen that, when $R_3 < R_c < R_4$ these two steps energies are different but become equal when $R_2 < R_c < R_3$ in which case

$$E_{step}^{2(100)\times(111)} = E_{step}^{3(100)\times(111)} = E(7,3) + E(10,5) - 3E(8,5)/2 - E(12,5)/2. \quad (20)$$

For the $p(111)\times(100)$ vicinal surfaces a similar calculation shows also that the two step energies are different when $R_3 < R_c < R_4$ but are equal when $R_2 < R_c < R_3$:

$$E_{step}^{2(111)\times(100)} = E_{step}^{3(111)\times(100)} = E(7,3) - 5E(9,3)/3 + E(10,5) + E(12,5) - 4E(12,6)/3. \quad (21)$$

Using Tables II and III the reader can verify that, when $R_2 < R_c < R_3$, the step energies of both $p(100)\times(111)$ and $p(111)\times(100)$ surfaces are not changed for $p > 3$.

Consequently for any semi-empirical potential of the form (12) including first and second nearest neighbors only, $\Delta f(\eta)$ has the triangular shape (Fig. 2) when relaxation is neglected and its sign is given by

$$\Delta E = E_S(311) - E_S(100) - E_S(111) \quad (22)$$

or

$$\Delta E = [E(7,3) + E(10,5)] - [E(8,5) + E(9,3)]. \quad (23)$$

This expression has an obvious physical meaning: ΔE arises from the difference of the sum of energies of, on the one hand, atoms belonging to the outer and inner step edges, and, on the other hand, of (100) and (111) surface atoms. From the previous subsection we know that the pair potential, when limited to second-nearest neighbors, does not contribute to ΔE which can be written as a function of the N-body part of the potential only. Noting that, since $g(R_1) = 1$, $\rho_i = \Sigma_{j\neq i} g(R_{ij}) = Z_1^i + Z_2^i g_2$ with $g_2 = g(R_2)$, ΔE is finally given by

$$\Delta E = [F(7+3g_2) - F(9+3g_2)] - [F(8+5g_2) - F(10+5g_2)]. \quad (24)$$

For all the existing potentials of the form (12) $F''(\rho) = d^2F/d\rho^2$ is positive. As a consequence $F(\rho-2) - F(\rho)$ is a decreasing function of ρ, therefore ΔE [and thus $\Delta f(\eta)$] is always positive in the whole domain. This common property of this class of potentials has a clear physical origin: the energy E_i of an atom i should decrease more and more slowly when its coordination increases towards the bulk coordination.[15,29] This clearly implies that $F''(\rho)$ must be positive. We have then proved that for *any* empirical potential of the general form (12) on a rigid lattice at 0 K and a cutoff radius $R_c < R_3$, *any* vicinal surface from (100) to (111) is *unstable* with respect to faceting.

(b) $p(\bar{1}11)\times(111)$-$p(111)\times(\bar{1}11)$ domain. We will limit ourselves to the values of R_c such that $R_c < R_3$ since the step energies cease to be a constant when $R_c > R_1$. Indeed for $p = 2$ and 3 they are not equal:

$$E_{step}^{2(111)\times(\bar{1}11)} = E(7,4) - 4E(9,3)/3 + E(11,4) - 2E(12,6)/3 \quad (25)$$

and

$$E_{step}^{3(111)\times(\bar{1}11)} = E(7,4) - 7E(9,3)/3 + E(9,4) + E(11,4) - 2E(12,6)/3. \quad (26)$$

It is easily shown that $E_{step}^{p(111)\times(\bar{1}11)}$ remains constant for $p \geqslant 3$ when first- and second-nearest neighbors are included and for $p \geqslant 2$ when interactions are limited to first-nearest neighbors.

As a consequence $\Delta f(\eta)$ has a triangular shape when $R_c < R_2$ and the vicinal surfaces between $(\bar{1}11)$ and (111) are unstable when Eq. (16) is fulfilled, i.e.,

$$[F(7) - F(9)] - [F(9) - F(11)] > 0 \quad (27)$$

since the pair potential V does not contribute to this condition. This inequality is always obeyed since, as explained above, $F(\rho-2) - F(\rho)$ is a decreasing function of ρ. In such a model, at least when atomic relaxation is neglected, the (011) surface is unstable relative to faceting into $(\bar{1}11)$ and (111) facets. Note that due to the very short range of the potential, the condition (27) gives also the instability relative to the missing row (1×2) reconstruction which has indeed $(\bar{1}11)$ and (111) microfacets.

When $R_c < R_3$, $\Delta f(\eta)$ is no more a simple triangle. However, it remains linear in the domain $(\bar{1}11)$-$(\bar{1}33)$, i.e., $\eta \in [-\sqrt{2}/2, -\sqrt{2}/6]$ and in the domain symmetrical with respect to $\eta = 0$. In these domains, the sign of $\Delta f(\sqrt{2}/6)$ [or $\Delta f(\eta)$] is given by

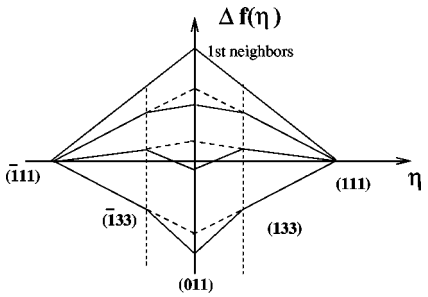

FIG. 4. Expected evolution of $\Delta f(\eta)$ (full lines) obtained with a semi-empirical potential including first- and second-nearest neighbors as a function of the energy contribution of the latter. $\Delta f(\eta)$ is lowered and may change sign depending on this contribution.

$$E_S(133)-3E_S(111)=E(7,3)+E(9,4)+E(11,4)-3E(9,3) \tag{28}$$

and it is expected to depend on the relative contributions of the first- and second-nearest neighbors to the energy. In addition the point $\Delta f(0)$ is not at the intersection of these two lines since the step energies are not the same for $p=2$ (011) and $p=3$ (133) [see Eqs. (25) and (26)]. It can be easily shown that $\Delta f(0)$ is below this intersection when

$$E_S(011)<E_S(133)-E_S(111) \tag{29}$$

or

$$[E(7,4)-E(9,4)]-[E(7,3)-E(9,3)]<0. \tag{30}$$

The pair part of the potential does not play any role in this condition which can be rewritten

$$[F(7+3g_2)-F(9+3g_2)] -[F(7+4g_2)-F(9+4g_2)]<0. \tag{31}$$

This inequality is always fulfilled since $F(\rho-2)-F(\rho)$ is a decreasing function of ρ.

As a conclusion, when $\Delta f(\eta)>0$ for $\eta\in[\pm\sqrt{2}/6, \pm\sqrt{2}/2]$ the (011) surface is stable relative to faceting into (111)/(111) facets if $\Delta f(0)$ is negative, i.e.,

$$E_S(011)-2E_S(111)=E(7,4)+E(11,4)-2E(9,3)<0. \tag{32}$$

This last condition may or may not not be fulfilled depending on the importance of second-nearest neighbors. When $\Delta f(\eta)<0$, $\Delta f(011)$ is below $\Delta f(133)$ (Fig. 4). Thus the semi-empirical potential (12) with $R_c<R_3$ cannot explain the faceting of the (011) surface into (133)/(133) facets observed for Ir,[30] at least when relaxation is neglected.

(c) $p(011)\times(111)$-$p(111)\times(011)$ domain. Limiting ourselves to $R_c<R_5$, we find that the step energies $E_{step}^{p(011)\times(111)}$ are independent of p in the whole range ($p\geqslant 2$) and equal to

$$\begin{aligned}E_{step}^{p(011)\times(111)}=&E(7,3,12,7)-3E(7,4,14,7)/2+E(9,4,16,7)\\&-3E(11,4,18,7)/2+E(11,4,19,9)\\&+E(12,6,19,9)-3E(12,6,20,11)/2\\&+E(12,6,22,11)-E(12,6,24,11)/2.\end{aligned} \tag{33}$$

Consequently, when $R_c<R_5$, $\Delta f(\eta)$ is linear between $\eta=0$ [(011) surface] and $\eta_c=\sqrt{2}/6$ [(133) surface].[31] It is easily seen from Tables IV and V that steps start to interact if the fifth neighbors are taken into account. We have seen above that $E_{step}^{(p+1)(111)\times(\bar{1}11)}$ (i.e., $E_{step}^{p(111)\times(011)}$) is a constant when $p\geqslant 2$ if $R_c<R_3$ but not when $R_c>R_3$. As a conclusion, in this domain, $\Delta f(\eta)$ has a triangular shape only when $R_c<R_3$ and, as shown above [Eqs. (29)–(32)], its sign is positive (see Fig. 3) which means that the corresponding vicinal surfaces are all unstable with respect to faceting into (011)/(111) facets.

Finally, if we compare the results obtained with a pair potential to those derived from usual potentials including an *N*-body part, we note that step interactions appear at a shorter cutoff distance in the latter case than in the former.

2. Application to vicinal surfaces of Cu

So far we have demonstrated general results on the stability of vicinal surfaces based on a rigid lattice description, both from pair potentials and *N*-body semi-empirical potentials. Most results were demonstrated under the assumption that the range of the potential is restricted to the first shells of neighbors, and it was often difficult to predict the exact behavior when the range of the potential is extended to further neighbors. Moreover, the effect of atomic relaxation was neglected. We will now consider a "real" case with a potential of the form given by Eq. (12) (see Ref. 10):

$$\begin{aligned}&E(R_1,\cdots R_i,\cdots)\\&\quad=A\sum_{i,j,j\neq i}(R_0/R_{ij})^p f_c(R_{ij})\\&\qquad-\xi\sum_i\left(\sum_{j\neq i}\exp[-2q(R_{ij}/R_0-1)]f_c(R_{ij})\right)^{\alpha},\end{aligned} \tag{34}$$

where R_{ij} is the distance between atoms i and j, R_0 is a reference distance that we take equal to the bulk nearest-neighbor spacing and $f_c(R)=1/\{1+\exp[(R-R_c)/\Delta]\}$ is a smooth cutoff function with a cutoff radius R_c and a characteristic length Δ that we set equal to 0.05 Å.

The parameters A, ξ, p, and q are fitted to the cohesive energy E_c and the three elastic constants (bulk and shear moduli B, C, and C'). The equilibrium equation gives a relation between the four parameters and the first-neighbor distance is fixed at the experimental value R_0. In the case of copper ($R_0=2.5526$ Å) we have found that with $\alpha=0.666$ we obtain an excellent fit (of the order of meV per atom) of the cohesive energy $E_c=-3.5$ eV/atom and of the bulk modulus, $B=10.470$ eV/atom, but the quality of the fit for

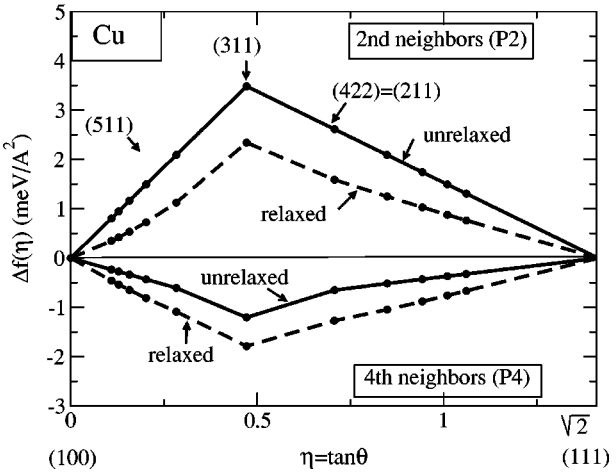

FIG. 5. $\Delta f(\eta)$ for Cu derived from the semi-empirical potential given in the text for two cutoff radii with and without relaxation for the (100)-(111) domain.

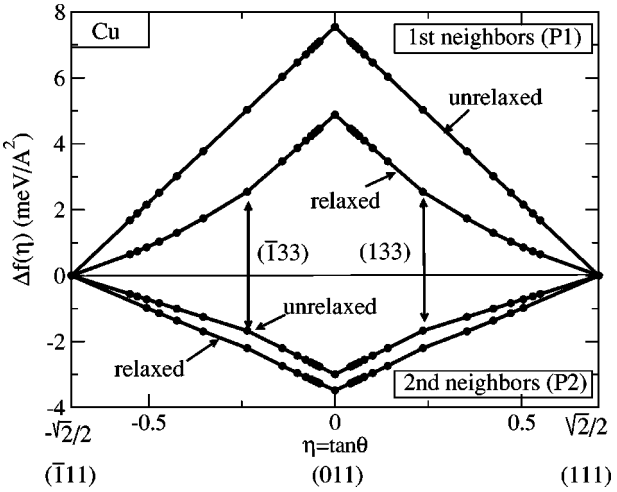

FIG. 6. Same as Fig. 5 for the $(\bar{1}11)$-(111) domain.

the two other elastic constants $C=6.046$ eV/atom and $C'=1.917$ eV/atom is strongly dependent on the cutoff radius. Moreover, the surface energies of the three low index surfaces (111), (001), and (011), even though not included in the fit, are better with $\alpha=0.666$ than with $\alpha=1/2$.

We have checked several sets of parameters, corresponding to different cutoff radii R_c, by comparing to experiment the result of the fit (in particular the two elastic constants C and C') and also the surface relaxation and the bulk phonon spectra.[12] It was found that the best set of parameters (called P_2) was obtained for a cutoff radius $R_c=4.02$ Å between second and third neighbors, the corresponding numerical values being $A=0.206$ eV, $\xi=1.102$ eV, $p=7.206$, $q=2.220$. However, to test the influence of R_c on the stability of vicinal surfaces we have also considered two other sets of parameters one, denoted as P_1, with a cutoff radius $R_c=3.08$ Å between first and second neighbors leading to $A=0.339$ eV, $\xi=1.447$ eV, $p=6.069$, $q=2.449$, and another one (P_4) with a cutoff radius $R_c=5.4$ Å between fourth and fifth neighbors, the corresponding parameters being $A=0.195$ eV, $\xi=1.021$ eV, $p=7.357$, $q=2.100$. In all cases the atomic structure of each surface has been fully relaxed using a conjugate gradient algorithm.

We will now examine the cases of the (100)-(111) domain. In Fig. 5 we have represented $\Delta f(\eta)$ with and without atomic relaxation for the two potentials P_2 and P_4. As expected from our previous analysis all vicinal surfaces between (100) and (111) are unstable for the P_2 potential the range of which is restricted to second neighbors (the potential P_1 leads qualitatively to the same results). However, we can see that the effect of farther neighbors is crucial since, with potential P_4, all vicinal surfaces between (100) and (111) become stable.

The case of the $(\bar{1}11)$-(111) domain is presented in Fig. 6 where we have shown $\Delta f(\eta)$ with and without atomic relaxation for the two potentials P_1 and P_2. Here again the range of the potential is crucial: as expected potential P_1 leads to an upward triangle and therefore an instability of all the vicinal surfaces [in particular the (011) surface is unstable with respect to faceting into (111) and $(\bar{1}11]$ facets], the inclusion of further neighbors totally modifies this picture since with potential P_2, $\Delta f(\eta)$ is negative and the (011) surface is stable. Moreover, as expected from analytical results (see Sec. II B 1 b) $\Delta f(0)$ is below the straight line defined by the (111) and (133) points and therefore all vicinals surfaces between (011) and (111) are unstable with respect to faceting into (011) and (111) orientations.

Finally one can see that atomic relaxation always acts in favor of a stabilization since the relaxation is larger on a vicinal surface that on a flat one. Typically the displacement of an atom relative to its lattice position is 0.035 and 0.037 Å inwards for a (100) and (111) surface atom, respectively, while it is also inwards but about 0.13 Å for an atom of the step edge using the potential P_2. A detailed study of this relaxation will be presented in a forthcoming paper.[32]. Nevertheless, this effect is rather small and in most cases it will not be large enough to modify the stability (or instability) of a surface. The only case where it could influence the stability is when $\Delta f(\eta)$ is positive but very small, the inclusion of atomic relaxation could then make $\Delta f(\eta)$ negative in some regions and positive in others leading to a more complex behavior. However, this situation is very unlikely and the inclusion of new effects (like that of vibrational energy) would also modify the picture in that specific case.

Let us discuss and summarize our results. From our analytical study and Figs. 5 and 6 it appears that the range of the potential plays an important role but it is difficult to draw general conclusions. In all cases considered here the effect of farther neighbors is to stabilize vicinal surfaces, however, including them will not automatically make vicinal surfaces stable, this crucially depends on their relative importance and therefore on the dependence of the functions $V(r)$ and $g(r)$ with distance [Eq. (12)]. The stability also depends on the relative importance of V with respect to $F(\rho)$ since when farther neighbors are included both terms are present in the energy balance. Moreover, in EAM and EMT potentials the embedding and pair parts are not necessarily purely attractive or purely repulsive, therefore even the sign of these terms is not known. Let us finally compare our results with those of

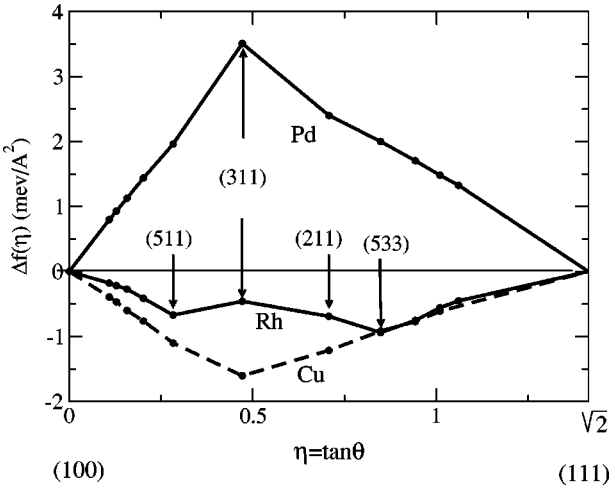

FIG. 7. $\Delta f(\eta)$ for Rh, Pd, and Cu from tight-binding calculations for the (100)-(111) domain.

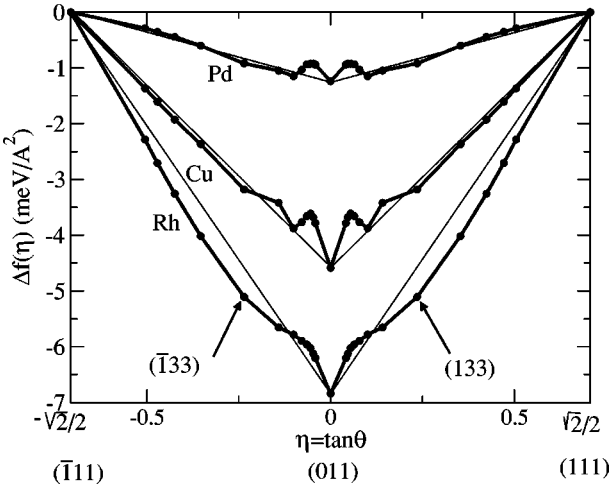

FIG. 8. Same as Fig. 7 for the $(\bar{1}11)$-(111) domain.

of Frenken and Stoltze.[33] These authors have calculated $\Delta f(\eta)$ for the fully relaxed (100) and (111) vicinal surfaces of Ag (and other metals) using an EMT potential with $R_3 < R_c < R_4$. However, the role played by the third neighbors is very small compared to that of first and second neighbors (to fix ideas, $g_1=1$, $g_2 \simeq 3\times10^{-2}$, $g_3 \simeq 3\times10^{-3}$). Our analysis shows that all the $\Delta f(\eta)$ curves calculated with a potential of type (12) and a cutoff radius $R_c < R_3$ will behave identically. In the case of their potential, even though third neighbors are included, their role is too small to have a significant influence. This explains the strong similarity between our results on relaxed Cu (Fig. 5) with potential P_2 and those of Frenken and Stoltze for Ag.

IV. STABILITY OF VICINAL SURFACES AT 0 K FROM TIGHT-BINDING CALCULATIONS

The potentials considered above have a common drawback: the energy of an atom i (on a rigid lattice) is completely fixed by its coordination numbers Z_N^i whereas it should also depend on the angular arrangement of its neighbors. This effect is accounted for in electronic structure calculations which, moreover, include long-range interactions (often oscillatory). These interactions, although small, may play a role in the very delicate energy balance which determines the stability of vicinal surfaces. In a recent paper[10] we calculated the step energies of various vicinal surfaces from a realistic tight-binding model for Rh, Pd, and Cu. The functions $\Delta f(\eta)$ derived from the results of this paper are plotted in Figs. 7 and 8 for the (100)-(111) vicinal surfaces and $(\bar{1}11)$-(111) vicinal surfaces, respectively.

As can be seen there is a great variety of shapes and the (100)-(111) domain is very different from the (111)-(111) domain. On the (100)-(111) domain we find that for Cu all vicinal surfaces are stable at 0 K while for Pd they are unstable. For Rh the situation is more complex: all vicinal surfaces are stable with respect to faceting into (100) and (111) surfaces, however, the curve presents two local minima at $\eta=\sqrt{2}/5$ [(511) surface] and $\eta=3\sqrt{2}/5$ [(533) surface] with a local maximum at $\eta=\sqrt{2}/3$ [(311) surface]. This means that the vicinal surfaces of orientation such that $\sqrt{2}/5 < \eta < 3\sqrt{2}/5$ are unstable relative to faceting into (511) and (533) orientations. This peculiar behavior is related to electronic step-step interactions which are repulsive for the (311) and (211) surfaces and attractive for (511) and (533) surfaces.[10] In the $(\bar{1}11)$-(111) domain the situation is rather different but some general features can, however, be drawn from Fig. 8: for the three considered elements the $(01\bar{1})$ surface is stable with respect to faceting into (111) and $(\bar{1}11)$ facets in agreement with experiment but it appears that vicinal surfaces $p(011)\times(111)$ are unstable for $p \geqslant 4$ since there is an inversion of curvature for $p \geqslant 4$. For copper and palladium there is a range of instability between $2(011)\times(111)$ or (133) and $4(011)\times(111)$ or (177) meaning that vicinal surfaces in this range are expected to facet into (133) and (177) orientations. For rhodium this instability is not present. Concerning the vicinal surfaces $p(111)\times(\bar{1}11)$ for $p>2$, Fig. 8 shows that they are stable for copper and rhodium but unstable for palladium. Unfortunately there are very few experimental data for this range of orientations, the only experimental result we are aware of is a study of Cu(133),[34] which is found to be stable in agreement with our findings. It would therefore be very interesting to have experimental studies of (011) vicinal surfaces with higher index ($p \geqslant 4$) to check the validity of our calculations.

V. FINITE TEMPERATURE EFFECTS ON THE STABILITY OF VICINAL SURFACES

So far all calculations were carried out at 0 K; we will now consider the influence of finite temperatures. There are two sources of variation of $f(\eta)$ with temperature: a purely statistical term $f_{stat}(T)$ due to the entropy S_{stat} gained by the meandering of steps regulated by the kink formation energy (ε_{kink}), therefore decreasing the free energy for step formation, and the vibrational free energy f_{vib} due to the vibrational motion of atoms. We then have

$$f(\eta,T) = f_0(\eta) + f_{stat}(\eta,T) + f_{vib}(\eta,T), \qquad (35)$$

where $f_0(\eta)$ is the static term independent of temperature. Actually f_{stat} is very difficult to calculate, it can, however, be evaluated analytically in a simple first-nearest neighbor Ising model for a free step on a (100) fcc surface[15] leading to

$$f_{stat}^{free}(\eta,T) = -\frac{k_B T}{A_0(\mathbf{n})} \ln\left[\coth\frac{\varepsilon_{kink}}{2k_B T}\right], \tag{36}$$

this expression being only valid when steps fluctuate independently of each other. Indeed, when the meandering of steps is large enough compared to the terrace width one must take into account the fact that steps cannot cross. This restriction decreases the configurational entropy and leads to an effective repulsion of the steps. One can formally write f_{stat} as the sum of two terms: f_{stat}^{free} and $f_{stat}^{nocross}$ which is the positive contribution due to the noncrossing condition.

For f_{stat} the low index surfaces do not contribute since the only allowed events that we consider are kink creation, therefore $\Delta f_{stat} = f_{stat}$. If we neglect the term due to the noncrossing condition Δf_{stat} has a simple downward triangular shape and the minimum is obtained for the intermediate vicinal surface corresponding to $\eta = \eta_c$ (or equivalently $p=2$) and is equal to

$$\Delta f_{stat}(\eta_c) = -k_B T \ln[\coth(\varepsilon_{kink}/2k_B T)]/[S_1(1+f_1)]. \tag{37}$$

This statistical contribution f_{stat} is obviously stabilizing vicinal surfaces and it varies rapidly with temperature. To fix ideas let us take the (100)-(311) domain [which corresponds to vicinal surfaces with (100) terraces] and a kink energy typically of 0.12 eV/atom for copper. One finds that $\Delta f_{stat}(\eta_c)$ is of the order of 10^{-9} eV/Å^2 at 100 K, 10^{-6} eV/Å^2 at 200 K, 0.05 meV/Å^2 at 300 K, and 0.5 meV/Å^2 at 500 K. Therefore at room temperature this statistical energetic contribution will be at most a few hundredths of meV for Cu and completely negligible in the case of elements with higher kink energies like rhodium and palladium. In any case f_{stat} has a negligible influence on the stability of vicinal surfaces.

The excess vibrational free energy has two contributions: the internal energy which dominates at low temperature and vanishes at high temperature and the entropy part which has the inverse behavior. This excess free energy has been evaluated in recent publications using a simple model of the Einstein type,[33,35,36] but in view of the rather delicate energy balance involved here it is more advisable to use a complete description of the phonon spectrum and include both the internal energy and the entropy part. Therefore we have calculated the vibrational free energy from precise phonon spectra based on the empirical potential P_2 which is known to reproduce very accurately the experimental data for the vibration spectra of bulk Cu and its low- and high-index surfaces.[12] Contrary to the statistical term the vibrational energy is obviously not zero on the flat surface and there is an important cancellation when calculating the difference of energy giving Δf_{vib}. On Figs. 9 and 10 we have represented Δf_{vib} for the two domains (100)-(111) and $(\bar{1}11)$-(111) at different temperatures from 0 to 500 K.

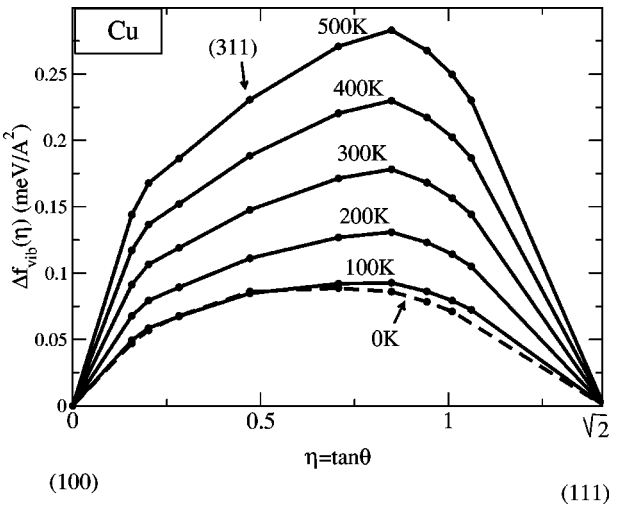

FIG. 9. $\Delta f_{vib}(\eta)$ for Cu in the (100)-(111) domain from potential P_2 as a function of temperature.

The main conclusion is that the order of magnitude of Δf_{vib} is approximately some tenths of meV/Å^2 and therefore in most cases it will have a negligible role on the stability. However, Δf_{stat} may become of the same order of magnitude as Δf_{vib} for temperatures above 300 K. One should also note that the shape of Δf_{vib} is very different for the two domains: it is positive for the (100)-(111) domain and consequently tends to destabilize vicinal surfaces, it is oscillatory with some positive and negative parts for the $(1\bar{1}1)$-(111) domain.

Finally, let us note that our results concerning the influence of the vibrational energy are in contradiction with those of Frenken and Stoltze,[33] since these authors claimed that phonons stabilize vicinal surfaces in the (100)-(111) domain. In their work they evaluated the role of phonons using a simplified Einstein model and neglected the internal energy, which is quite questionable at low temperatures. Moreover, in their evaluation of Δf_{vib} they used a formula similar to Eq. (23) but in which they only included the difference be-

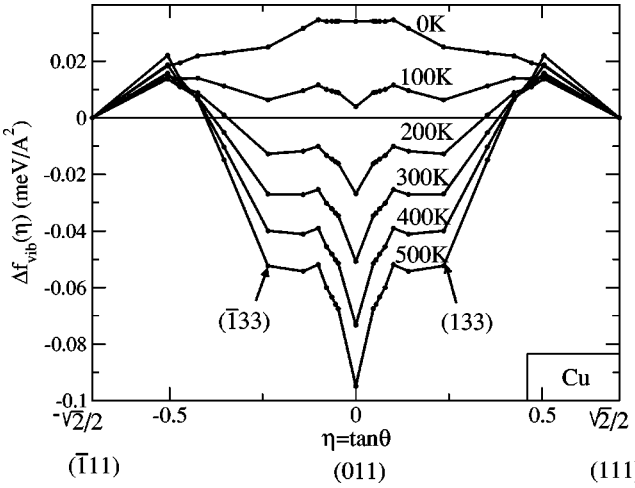

FIG. 10. $\Delta f_{vib}(\eta)$ for Cu in the $(\bar{1}11)$-(111) domain from potential P_2 as a function of temperature.

tween the outer edge and a (111) surface atom, i.e., $E(7,3)-E(9,3)$. Our analytical calculations [Eq. (23)] show that at least another term should imperatively be considered, namely $E(10,5)-E(8,5)$ arising from the difference between the inner edge and a (100) surface atom. These two terms have opposite signs and are expected to be of the same order of magnitude. This explains why not only the order of magnitude of Frenken and Stoltze estimation is too large (meV instead of tenths of meV) but even the sign is wrong since we find that phonons tend to destabilize vicinal surfaces, at least for Cu, in the (100)-(111) domain whereas the influence of phonons can be stabilizing in some regions and destabilizing in some others in the $(1\bar{1}1)$-(111) domain.

VI. CONCLUSION

In this paper we have investigated the implications of different approaches for calculating the surface energies on the stability of vicinal surfaces with respect to faceting. We have shown that, although effective pair potentials are useful to estimate step energies,[10,14] this method is not precise enough to determine the stability of vicinal surfaces. First, in this model, the stability would be governed by pair potentials beyond first-nearest neighbors, at least. As emphasized in Ref. 10 the sign of these terms is not known with certainty since it depends on the surface energy data base used to determine them. When surface energies are calculated from semi-empirical potentials, we have seen that the results depend on the cutoff distance chosen for the interatomic interactions and of the importance of farther neighbors compared with first-nearest neighbors. Moreover, the shape of $\Delta f(\eta)$ remains schematic, even when atomic relaxation is included. In addition, pair potentials, as well as *N*-body semi-empirical ones, have a common drawback: they only depend on the interatomic distances and not on the angular arrangement of atoms. This latter effect is small in metals. However, it cannot be neglected in view of the delicate energy balance which governs the stability of vicinal surfaces with respect to faceting. On the contrary, electronic structure calculations take this effect into account and open up the possibility of a large variety of behaviors, including a possible faceting of a vicinal surface into two different vicinal surfaces. Such a phenomenon is a consequence of electronic oscillatory step-step interactions. Finally temperature effects are found to be most often negligible, at least up to room temperature.

APPENDIX A: FACETING CONDITION AND HERRING GEOMETRICAL CONSTRUCTION

In this appendix we show the equivalence between the geometrical construction of Herring and the simpler faceting criterion derived in Sec. II. Let us recall the Herring construction.[13] One starts from the γ plot in polar coordinates. An example of a γ plot, obtained for copper from our tight-binding calculations, is given in Fig. 11. Its most striking feature is the existence of well defined cusps in some directions, namely (111), (100), and (011). The more close packed the surface, the deeper the cusp. This appears clearly in Fig. 11 where the direction corresponding to the (111)

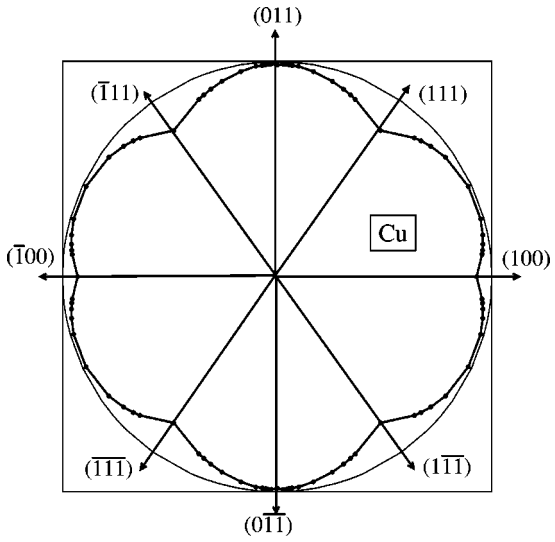

FIG. 11. γ plot of Cu for the orientations studied in the main text.

surface has a more pronounced cusp than the (100) direction, while that of the (011) direction is hardly visible. We consider a schematic case with a strong anisotropy, for the sake of clarity, as shown in Fig. 12. First we construct the plane π, perpendicular to the radius vector of the γ plot and tangent to the Wulff equilibrium shape at point *I*. Let us call *H* the projection of the center of the γ plot *O*, on π, and set $\gamma_f = OH$. When the radius vector scans all the γ plot the point *H* scans a surface that we will call Γ. From Herring criterion, the surface is unstable with respect to faceting if the surface Γ is inside the γ plot.

We will now recast this geometrical construction into the more straightforward one derived in Sec. II. Let us first calculate $\gamma_f(\theta)$:

$$\gamma_f(\theta) = OH = OI\cos(\theta_\perp - \theta) \tag{A1}$$

with $OI = \gamma(\mathbf{n}_1)/\cos(\theta_\perp)$, therefore we have

$$\gamma_f(\theta) = \frac{\cos(\theta_\perp - \theta)}{\cos(\theta_\perp)}\gamma(\mathbf{n}_1). \tag{A2}$$

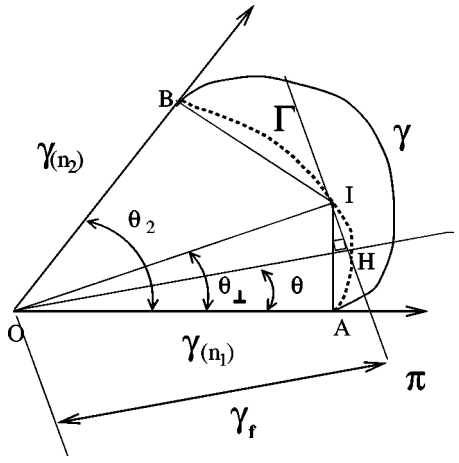

FIG. 12. The Herring construction.

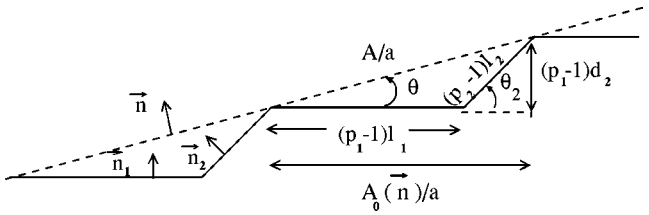

FIG. 13. Cut of a vicinal surface with terraces of orientations $\mathbf{n}_1$ when $p_2=2$ and $\mathbf{n}_2$ when $p_1=2$.

As seen from Sec. II, the relevant function is $\gamma(\theta)/\cos(\theta)$. Let us then calculate

$$\frac{\gamma_f(\theta)}{\cos(\theta)}=\gamma(\mathbf{n}_1)+[\gamma(\mathbf{n}_1)\tan\theta_\perp]\tan\theta. \tag{A3}$$

Actually OI has two equivalent expressions whether the origin of the angles are the directions $\mathbf{n}_1$ or $\mathbf{n}_2$, one gets

$$OI=\frac{\gamma(\mathbf{n}_1)}{\cos(\theta_\perp)}=\frac{\gamma(\mathbf{n}_2)}{\cos(\theta_2-\theta_\perp)} \tag{A4}$$

which allows one to derive an expression for $\tan\theta_\perp$:

$$\tan\theta_\perp=\frac{\gamma(\mathbf{n}_2)}{\gamma(\mathbf{n}_1)\sin\theta_2}-\frac{1}{\tan\theta_2}. \tag{A5}$$

Substituting Eq. (A5) for $\tan\theta_\perp$ into Eq. (A3) yields

$$\frac{\gamma_f(\theta)}{\cos(\theta)}=\left(1-\frac{\tan\theta}{\tan\theta_2}\right)\gamma(\mathbf{n}_1)+\left(\frac{\tan\theta}{\tan\theta_2}\right)\frac{\gamma(\mathbf{n}_2)}{\cos\theta_2}. \tag{A6}$$

Comparing Eq. (A6) with the inequality (4) the faceting condition can be written

$$\gamma(\theta)>\gamma_f(\theta). \tag{A7}$$

Thus the faceting condition given by Herring construction is equivalent to the inequality (4).

APPENDIX B:

Let us consider the stepped surface of orientation $\mathbf{n}$ shown in Fig. 13. The planes of normal $\mathbf{n}_1$ are taken as the origin of angles, i.e., $\theta=(\mathbf{n}_1,\mathbf{n})$, $\theta_2=(\mathbf{n}_1,\mathbf{n}_2)$. The spacing of atomic rows parallel to the step edges is denoted as l_1 (l_2) in the face of normal $\mathbf{n}_1$ ($\mathbf{n}_2$), d_1 is the interplanar spacing along direction $\mathbf{n}_1$, and a the interatomic spacing along the rows. p_1 and p_2 denote the numbers of atomic rows in each facet including the inner edge. All vicinal surfaces with monoatomic steps encountered in the domain $[0,\theta_2]$ are of this type with

$$\infty>p_1\geqslant 2;\quad p_2=2\quad \text{when}\quad 0<\theta\leqslant\theta_c,$$

$$p_1=2;\quad 2\leqslant p_2<\infty\quad \text{when}\quad \theta_c<\theta\leqslant\theta_2.$$

We want to prove Eq. (5) starting from [see Eq. (4)]

$$\Delta f(\mathbf{n})=\frac{\gamma(\mathbf{n})}{\cos\theta}-\left(1-\frac{\tan\theta}{\tan\theta_2}\right)\gamma(\mathbf{n}_1)-\left(\frac{\tan\theta}{\tan\theta_2}\right)\frac{\gamma(\mathbf{n}_2)}{\cos\theta_2}, \tag{B1}$$

where $\gamma(\mathbf{n})$ is the surface energy per unit area of a surface of orientation $\mathbf{n}$. Let us denote as A, A_1, and A_2 the areas of the unit cells of the planes with normals $\mathbf{n}$, $\mathbf{n}_1$, and $\mathbf{n}_2$, respectively, and $A_0(\mathbf{n})=A\cos\theta$ the projection of A on the plane of orientation $\mathbf{n}_1$. The following relations hold:

$$A_1=al_1, \tag{B2}$$

$$A_2=al_2=\frac{ad_1}{\sin\theta_2}, \tag{B3}$$

$$\tan\theta=\frac{(p_2-1)d_1\tan\theta_2}{(p_2-1)d_1+(p_1-1)l_1\tan\theta_2}. \tag{B4}$$

Introducing the surface energies per surface atom $E_s(\mathbf{n})$ into Eq. (B1) gives

$$\Delta f(\mathbf{n})=\frac{E_s(\mathbf{n})}{A\cos\theta}-\left(1-\frac{\tan\theta}{\tan\theta_2}\right)\frac{E_S(\mathbf{n}_1)}{A_1}-\left(\frac{\tan\theta}{\tan\theta_2}\right)\frac{E_S(\mathbf{n}_2)}{A_2\cos\theta_2}. \tag{B5}$$

Substituting Eqs. (B2), (B3), and (B4) for A_1, A_2, and $\tan\theta$ into Eq. (B5) yields

$$\Delta f(\mathbf{n})=[E_S(\mathbf{n})-(p_1-1)E_S(\mathbf{n}_1)-(p_2-1)E_S(\mathbf{n}_2)]/A_0(\mathbf{n}). \tag{B6}$$

[1] P. Gambardella, M. Blanc, K. Kuhnke, K. Kern, F. Picaud, C. Ramseyer, C. Girardet, C. Barreteau, D. Spanjaard, and M.C. Desjonquères, Phys. Rev. B **64**, 045404 (2001).

[2] S. Rousset, F. Pourmir, J.M. Berroir, J. Klein, J. Lecoeur, P. Hecquet, and B. Salanon, Surf. Sci. **422**, 33 (1999).

[3] J. Frohn, M. Giesen, M. Poensgen, J.F. Wolf, and H. Ibach, Phys. Rev. Lett. **67**, 3543 (1991).

[4] W.W. Pai, J.S. Ozcomert, N.C. Bartelt, T.L. Einstein, and J.E. Reutt-Robey, Surf. Sci. **307-309**, 747 (1994).

[5] M. Giesen and G. Schulze Icking-Konert, Surf. Rev. Lett. **6**, 25 (1999).

[6] M. Giesen, Prog. Surf. Sci. **68**, 1 (2001), and references therein.

[7] L. Masson, L. Barbier, and J. Cousty, Surf. Sci. **317**, L1115 (1994).

[8] A.E. Carlsson, Solid State Phys. **43**, 1 (1990), and references therein.

[9] S. Papadia, M.C. Desjonquères, and D. Spanjaard, Phys. Rev. B **53**, 4083 (1996).

[10] F. Raouafi, C. Barreteau, M.C. Desjonquères, and D. Spanjaard, Surf. Sci. **482-485**, 1413 (2001); **505**, 183 (2002).

[11] M.C. Desjonquères, D. Spanjaard, C. Barreteau, and F. Raouafi, Phys. Rev. Lett. **88**, 056104 (2002).

[12] F. Raouafi, C. Barreteau, M.C. Desjonquères, and D. Spanjaard, Surf. Sci. **507-510,** 748 (2002).

[13] C. Herring, Phys. Rev. **82**, 87 (1951)

[14] L. Vitos, H.L. Skriver, and J. Kollár, Surf. Sci. **425**, 212 (1999).

[15] M.C. Desjonquères and D. Spanjaard, *Concepts in Surface*

Physics, 2nd edition (Springer-Verlag, Berlin, 1996).
[16] P. Stoltze, J. Phys.: Condens. Matter **6**, 9495 (1994).
[17] K.W. Jacobsen, P. Stoltze, and J.K. Norskov, Surf. Sci. **366**, 394 (1996).
[18] M.S. Daw, S.M. Foiles, and M.I. Baskes, Mater. Sci. Rep. **9**, 251 (1993), and references therein.
[19] F. Ercolessi, M. Parrinello, and E. Tosatti, Philos. Mag. A **58**, 213 (1988).
[20] F. Ducastelle, J. Phys. (France) **31**, 1055 (1970).
[21] M.W. Finnis and J.E. Sinclair, Philos. Mag. A **50**, 45 (1984).
[22] V. Rosato, M. Guillopé, and B. Legrand, Philos. Mag. A **59**, 321 (1989).
[23] A.P. Sutton and J. Chen, Philos. Mag. Lett. **61**, 139 (1990).
[24] J. Guevara, A.M. Llois, and M. Weissmann, Phys. Rev. B **52**, 11 509 (1995).
[25] B. Lang, R.W. Joyner, and G.A. Somorjai, Surf. Sci. **30**, 440 (1972).
[26] A. Gaussmann and N. Kruse, Surf. Sci. **266**, 46 (1992).
[27] L. Vitos, B. Johansson, H.L. Skriver, and J. Kollár, Comput. Mater. Sci. **17**, 156 (2000).
[28] It is worth noticing that, in the pair potential model, steps start to interact when R_c is equal or larger than the smallest bond joining two atoms belonging to two consecutive outer (or inner) step edges for $p=3$.
[29] I.J. Robertson, M.C. Payne, and V. Heine, Europhys. Lett. **15**, 301 (1991).
[30] J. Kuntze, S. Speller, and W. Heiland, Surf. Sci. **402-404**, 764 (1998).
[31] This means also that in the study of the $(\bar{1}11)$-(111) domain with $R_c<R_3$, the point (011) and (133) [and (011) and $(1\bar{3}3)$] are connected by a straight line.
[32] C. Barreteau, F. Raouafi, M.C. Desjonquères, and D. Spanjaard, Surf. Sci. (to be published).
[33] J.W.M. Frenken and P. Stoltze, Phys. Rev. Lett. **82**, 3500 (1999).
[34] B. Loisel, Ph.D. thesis, University of Paris 7 (1989).
[35] H.P. Bonzel and A. Emundts, Phys. Rev. Lett. **84**, 5804 (2000).
[36] H.J.W. Zandvliet, O. Gurlu, and B. Poelsema, Phys. Rev. B **64**, 073402 (2001).